PREDICTED CHANGES IN THE KNEE ADDUCTION TORQUE DUE TO GAIT MODIFICATIONS

By

KELLY L. ROONEY

A THESIS PRESENTED TO THE GRADUATE SCHOOL
OF THE UNIVERSITY OF FLORIDA IN PARTIAL FULFILLMENT
OF THE REQUIREMENTS FOR THE DEGREE OF
MASTER OF SCIENCE

UNIVERSITY OF FLORIDA

2005

ACKNOWLEDGMENTS

I would like to thank my committee chair, Dr. B.J. Fregly, for his guidance and support. I would also like to thank my other committee members, Dr. Raphael Haftka and Dr. Malisa Sarntinoranont, for their suggestions and time.

I greatly appreciate all of the support and friendship provided by the other students in the Computational Biomechanics Lab. Specifically, I appreciate Jeff for contributions to my research, Zhao Dong and Yi-chung for Chinese lessons, and Langston and Carlos for moral support and encouragement.

I would also like to thank my friends from the Tri-Gators and Roller Hockey Team for providing me with an athletic escape from the academic world.

Finally, I would like to thank Bernd for his personal support throughout the years.

TABLE OF CONTENTS

LIST OF TABLES

LIST OF FIGURES

Abstract of Thesis Presented to the Graduate School
of the University of Florida in Partial Fulfillment of the
Requirements for the Degree of Master of Science

PREDICTED CHANGES IN THE KNEE ADDUCTION
TORQUE DUE TO GAIT MODIFICATIONS

Kelly L. Rooney

May 2005

Chair: Benjamin J. Fregly
Major Department: Biomedical Engineering

Dynamic optimizations capable of predicting novel gait motions have great potential for addressing clinically significant problems in orthopedics and rehabilitation. This study evaluates gait modifications as an alternative to surgery for treating medial compartment knee osteoarthritis. Researchers developing forward dynamic optimizations of gait for such applications face significant challenges that may be resolved by implementing an inverse dynamic approach. This study used Fourier coefficients, which defined the motion and ground reaction torque curves, as kinematic design variables with an inverse dynamics optimization to predict novel motions. The cost function, minimized by a nonlinear least squares optimization function, included the left knee adduction torque and several reality constraints. Two sets of prediction optimizations were performed to evaluate the effect of foot placement on the knee adduction torque. The first set of prediction optimizations, which allowed leg torques to change without limit, resulted in motions with similar kinematic changes that reduced the knee adduction torque (72% average decrease) regardless of the foot path. The second set, which tracked

experimental leg torques, also resulted in the knee adduction torque being reduced for all cases (45% average decrease), but to a lesser degree. The optimizations suggest that novel movement modifications can have a significant effect (more than a high tibial osteotomy surgery) on reducing the peak knee adduction torque during gait.

CHAPTER 1
BACKGROUND

Osteoarthritis

The most common type of arthritis, known as osteoarthritis, affects 15 million people in the United States today according to the 2004 National Arthritis Meeting Report. This degenerative disease occurs when the cartilage, or cushioning, between bones breaks down due to uneven loading and excessive wear. Over time, cartilage in a joint may be completely worn away leaving painful bone on bone contact. Osteoarthritis is most common in the large weight bearing joints such as the hips and knees.

Knee Adduction Torque

Most patients who suffer from knee osteoarthritis have loss of cartilage in the medial compartment of the knee joint. This is due to the knee adduction torque, which results from the way the human body is constructed. When a person is standing on one leg, their center of mass falls medially, or inside, of the standing leg. The weight of the body acts to adduct the knee. Adduction causes the medial compartment of the knee to be forced together and the lateral knee compartment to be pulled apart. As a person walks, the knees repeatedly go through cycles of this uneven loading. Over time this will cause breakdown of the medial compartment cartilage. These effects are multiplied in patients with a varus (bow-legged) alignment.

High Tibial Osteotomy

In order to stop this breakdown of essential cartilage, a patient may undergo a high tibial osteotomy surgery. This procedure removes a wedge of bone from the tibia, or shin

bone, in order to correct a varus, or bow-legged, alignment. The forces in the knee are shifted laterally in order to move the pressure from the damaged cartilage to the healthy tissue.

Motion Capture

The motion data of a patient is collected in a gait lab using high-speed, high-resolution cameras. Spheres covered with reflective tape are placed on all segments of the patient's body. The cameras record the location of these markers over time. The marker data is used to create a computer model by calculating the location and orientation of the joints with respect to the markers. The movement of the markers throughout the gait cycle is used to calculate the motion of the joints.

Dynamic Simulations

The computer model of the patient's gait, or walking, cycle, is used to perform dynamic simulations. The modeling software creates the equations of motion based on the model structure and joint motions provided. These equations are used to solve dynamic simulations. Two types of dynamic simulations are discussed in this paper. Inverse dynamics, as the name suggests, occurs in the opposite order of real life events. Given the motion of a model, inverse dynamics is used to calculate the forces and torques that would produce that motion. Forward dynamics on the other hand occurs in the natural order. Forces and torques are input to calculate the resulting motions.

Optimization

An optimization is a mathematical method used to find the best solution to a problem. The important components of an optimization are design variables, a cost function, and constraints. The design variables are the values that are changed in order to search for the solution. The optimizer seeks to find the values of the design variables that

will minimize or maximize a cost function. Constraints are boundaries that cannot be crossed while searching for the optimal solution.

CHAPTER 2
INTRODUCTION

Dynamic optimizations capable of predicting novel gait motions have great potential for addressing clinically significant problems in orthopedics and rehabilitation (Delp *et al*., 1990; Delp *et al*., 1996; Pandy, 2001). In orthopedics, an optimization may be valuable to predict the outcome of certain procedures given various combinations of surgical parameters. For example, Cerebral Palsy patients often have muscles lengthened or redirected to improve gait coordination (Arnold *et al.*, 2001). A predictive model may demonstrate how such changes affect the entire body rather than just one or two joints spanned by the altered muscle. As another example, tibial osteotomy patients may have lower leg alignment corrected to relieve knee pain due to osteoarthritis. Researchers have investigated the relationship between dynamic gait measurements and clinical outcome, with the peak knee adduction moment being identified as an important clinical marker (Andriacchi, 1994; Hurwitz *et al.*, 1998; Prodromos *et al.*, 1985;Sharma *et al.*, 1998; Wang *et al.*, 1990). A model could help define the optimal amount of correction by predicting the post surgery knee forces and torques throughout the entire gait cycle. In rehabilitation, a predictive gait model could permit the development of novel rehabilitation procedures that may be difficult to identify experimentally.

Researchers developing forward dynamic optimizations of gait for such applications face two significant challenges. The first problem is instability of the repeated forward simulations performed during the optimization process. During gait, the body can be viewed as an inverted pendulum where the mass of the upper body swings

over a foot fixed to the ground. Without constraints or feedback control, the torso will quickly fall over in forward dynamic simulations driven only by torque actuators (Winter, 1990). Others have used muscles to overcome this instability (Gerristen *et al*., 1998). Muscles act as inherent stabilizers due to their force-length and force-velocity properties. The second obstacle is large computational cost associated with repeated numerical integration of the equations of motion for full-body, three-dimensional (3D) gait models. Previous investigations required parallel processing to complete such large-scale optimizations (Anderson and Pandy, 2001).

Both problems associated with a forward dynamic optimization may be resolved by implementing an inverse dynamic approach. With forward dynamic optimization, design variables are placed on the torques and the equations of motion are integrated to predict motion. However, if the design variables are instead placed on the motion, an inverse dynamics approach can be used to predict the resulting motion and loads similar to forward dynamic optimization. Contrary to forward dynamics, the inverse approach does not have stability problems nor does it require costly numerical integrations.

This study evaluates gait modifications as an alternative to surgery for treating medial compartment knee osteoarthritis. The specific goal was to predict the influence of foot position (i.e., toe out and wider stance) on the peak knee adduction moment. The predictions were developed using inverse dynamic optimization of a 27 degree-of-freedom (DOF), full-body gait model. The optimizations sought to minimize the peak knee adduction moment and were performed under two conditions. The first allowed the optimizer to vary the joint torques without limit, while the second sought to change the

nominal torques as little as possible. Novel movement modifications may have a significant affect on reducing the peak knee adduction moment during gait.

CHAPTER 3
METHODS

Experimental Data Collection

Gait data were collected from a single adult male using a HiRes Expert Vision System (Motion Analysis Corp., Santa Rosa, CA) with institutional review board approval. Surface marker data of a modified Cleveland Clinic marker set were collected at 180Hz for static and dynamic trials. The static trials were used to define segment coordinate systems and the locations of the markers within those coordinate systems. Dynamic joint trials were used to define the location and orientations of the joints. Dynamic gait trials provided the marker location data for an entire gait cycle. Two force plates (Advanced Mechanical Technology, Inc., Watertown, MA) recorded the ground reaction forces and torques of each foot about the electrical center of the respective force plate. The raw data were filtered using a fourth-order, zero phase-shift, low pass Butterworth Filter with a cutoff frequency of 6 Hz.

Dynamic Gait Model Development

Identical 3D, full body dynamic models were developed using Autolev (Online Dynamics, Inc., Sunnyvale, CA), a symbolic manipulator for engineering and mathematical analysis, and Software for Interactive Musculoskeletal Modeling (SIMM, Motion Analysis Corporation, Santa Rosa, CA). The Autolev model was designed for patient specific motion analysis and provides direct access to the equations of motion. The SIMM model provided visualization of the motion, and allows for the computation of muscle forces. Two models were necessary to validate the inverse dynamic approach

did not contain programming flaws. The models consist of 14 segments linked by 27 DOFs including gimbal, universal, and pin joints. Similar to Pandy's (2001) model structure, 3 translational and 3 rotational DOFs express the movement of the pelvis in a Newtonian reference frame. The remaining lower body DOFs include 3 DOF hip joints, 1 DOF knee joints, and 2 DOF ankle joints. The upper body DOFs include a 3 DOF back joint, 2 DOF shoulder joints, and 1 DOF elbow joints. (**Error! Reference source not found.**).

Inverse dynamic analysis was performed on both full-body models using the state-space form of the equations of motion. Consequently, 27 control forces and torques were calculated from the experimentally determined joint kinematics and ground reaction quantities. All forces and torques calculated by the two models were identical to within round-off error, providing a check on the dynamical equation formulation. An additional degree of freedom in the model, prescribed to produce no motion, was used to calculate the left knee adduction torque. External forces and torques acting on the pelvis were also calculated, since the model's position and orientation with respect to the ground frame are defined by a 6 DOF joint between the ground and pelvis. In reality there are no external forces or torques acting on the pelvis segment. Any non-zero force and/or torque found at this joint represents error in the model and/or data.

Dynamic Model Parameter Tuning

A nonlinear least squares optimization was performed using Matlab (The Mathworks, Natick, MA) to find model parameters, joint kinematics, and ground reactions to create a nominal data set consistent with the dynamical equations and the experimental gait data. The goal of this optimization was to alter the experimental data as little as possible while adjusting selected model parameters, smoothing the inverse

dynamic torques, and driving the external pelvis forces and torques close to zero. The optimization design variables were selected joint parameters (positions and orientations in the body segments), body segment parameters (masses, mass centers, and moments of inertia), and parameters defining the joint trajectories. A penalty was placed on changes to the body segment parameters in order to minimize the differences between the optimized data and the experimental data.

Movement Prediction via Inverse Dynamic Optimization

Motion and ground reaction torque curves were parameterized by a combination of polynomial and Fourier terms. The coefficients served as design variables for an inverse dynamics optimization used to predict novel motions. To accurately match the experimental data (Table 1), 8 harmonics and a cubic polynomial were needed for each DOF and ground reaction. The motion curves were differentiated to calculate velocities and accelerations. The right and left ground reaction forces and torques measured in the ground frame were applied to the respective feet. The resulting kinematics were used to calculate the corresponding joint forces and torques.

Table 1: RMS errors between the Fourier fit curves and experimental data.

Ground Reaction Forces (N)	Ground Reaction Torques (Nm)	Translations (cm)	Rotations (deg)
4.13	0.750	0.0257	0.173

The inverse dynamic optimization used the Matlab nonlinear least squares algorithm “lsqnonlin” and minimized the left knee adduction torque subject to several reality constraints implemented via a penalty method (Equation 1):

$$\min \sum_{f=1}^{100}\left\{T_{L\,Add}^{2}+w_{Kinematic}\left[\sum_{j=1}^{3}(\Delta q_{Trunk}^{2})_{j}+\sum_{j=1}^{2}(\Delta q_{Pelvis}^{2})_{j}+\sum_{s=1}^{2}\left(\sum_{j=1}^{6}(\Delta q_{Foot}^{2})_{sj}\right)\right]+\right.$$
$$w_{Kinetic}\left[\sum_{j=1}^{6}(\Delta T_{Pelvis}^{2})_{j}+\sum_{s=1}^{2}\left(\sum_{j=1}^{3}(\Delta T_{Hip}^{2})_{sj}+(\Delta T_{Knee}^{2})_{s}+\sum_{j=1}^{2}(\Delta T_{Ankle}^{2})_{sj}\right)\right]+ \tag{1}$$
$$\left.w_{CoP}\sum_{s=1}^{2}\left(\sum_{j=1}^{2}(e_{CoP}^{2})_{sj}\right)\right\}$$

where

f refers to time frame (1 through 100)

j refers to translational or rotational joint axis number (maximum value depends on number of prescribed joint axes for the specified anatomic joint)

s refers to side (1 for left, 2 for right)

$w_{Kinematic} = 2$, $w_{Kinetic} = 2$, and $w_{CoP} = 20$ are weight factors determined by trial and error

$T_{L\,Add}$ is left knee adduction torque

Δq_{Trunk} is change in trunk x, y or z rotation (j = 1 to 3) away from its nominal value measured with respect to the lab frame

Δq_{Pelvis} is change in pelvis x or z translation (j = 1, 2) away from its nominal value measured with respect to the lab frame

Δq_{Foot} is change in foot x, y or z translation or rotation (j = 1 to 6) away from its nominal value measured with respect to the lab frame

ΔT_{Pelvis} is change in external pelvis x, y or z force or torque (j = 1 to 6) away from its nominal value (close to zero) expressed in the lab frame

ΔT_{Hip} is change in hip flexion/extension, abduction/adduction, or inertial/external rotation torque (j = 1 to 3) away from its nominal value

ΔT_{Knee} is change in knee flexion/extension torque away from its nominal value

ΔT_{Ankle} is change in ankle flexion/extension or inversion/eversion torque (j = 1, 2) away from its nominal value

e_{CoP} is error in the center of pressure x or z location (j = 1, 2) beyond the outer edge of the foot

The predicted motion was forced to follow a prescribed foot path. This constraint allowed for the evaluation of various foot placements by altering the foot path to be matched. The trunk orientations were constrained to match the experimental orientations in order to avoid a motion where the model leaned over unrealistically. The transverse plane translations were also constrained to match the experimental translations. This constraint prevented the model from swinging a hip out laterally in such a way that an actual person may lose balance. The pelvis residual forces and torques were minimized because any non-zero residual would be an error. Because the ground reaction torques were design variables, the centers of pressure of the resultant right and left ground reaction forces were constrained to pass through the respective feet.

Two sets of prediction optimizations were performed to evaluate the effect of foot placement on the knee adduction torque. The first set allowed the leg torques to change without limit (i.e., ΔT_{Hip}, ΔT_{Knee}, and ΔT_{Ankle} were removed from Eq. (1)), while the second set minimized the difference between the experimental and optimized leg torques. Five cases were run within each set to evaluate the combinations of toeing out or changing stance width. The first case sought to match the experimental foot path. The remaining cases included all combinations of toeing out $\pm$15° and changing the stance

width by ±5 cm (Table 2). For each combination of foot path within each set of prediction optimization, the kinematic and kinetic changes were compared.

Table 2. Various foot path cases tested for effect on knee adduction.

	Foot Path Changes	
Case	**Toe Out (degrees)**	**Stance Width (cm)**
1	0	0
2	15	5
3	15	-5
4	-15	5
5	-15	-5

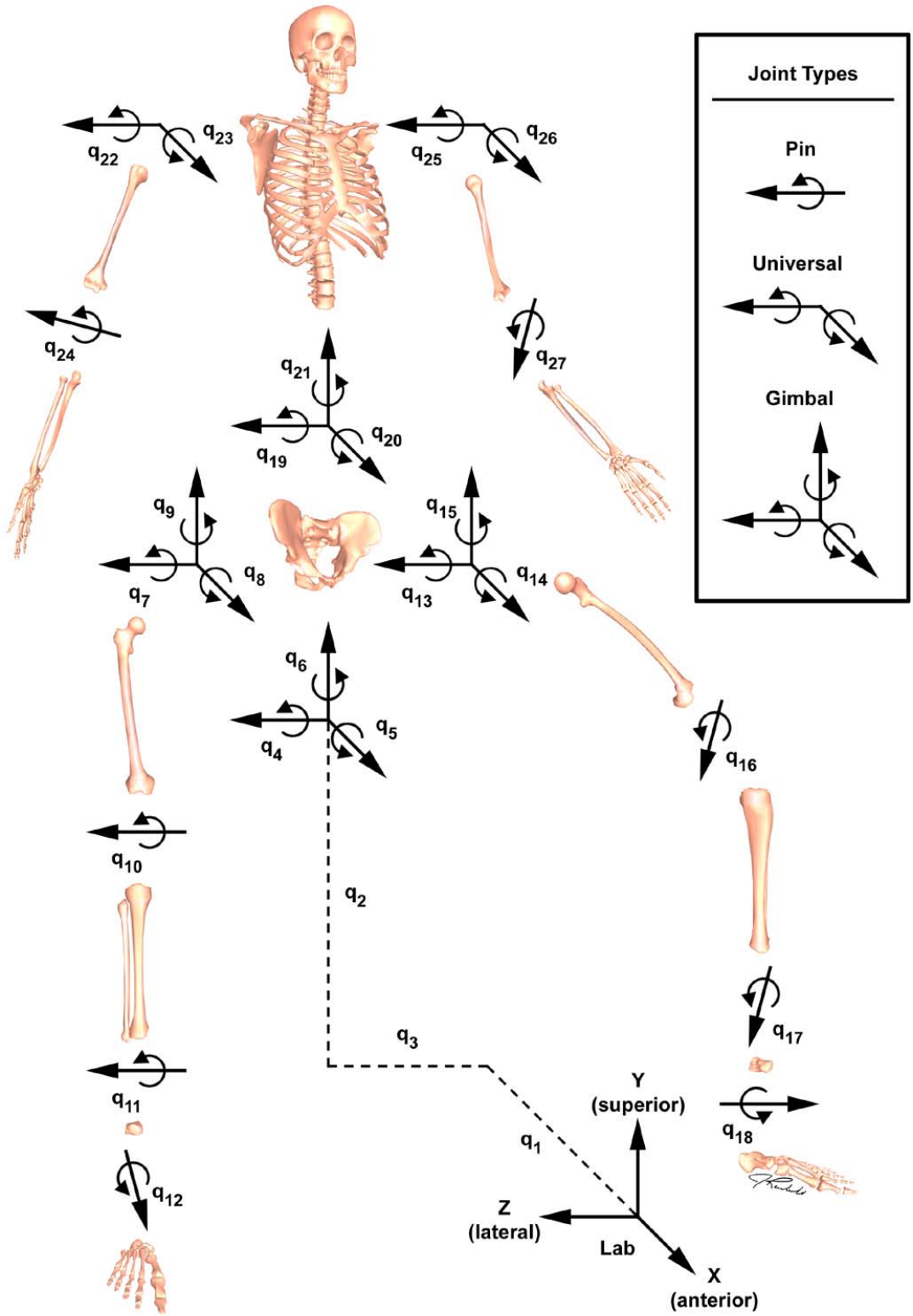

Figure 1. The 3D, 14 segment, 27 DOF full-body kinematic model linkage joined by a set of gimbal, universal, and pin joints.

CHAPTER 4
RESULTS

Optimizations without Experimental Leg Torque Tracking

The first set of prediction optimizations allowing leg torques to change without limit resulted in motions with similar kinematic changes that reduced the knee adduction torque (72% average decrease) regardless of the foot path (Figure 2). The kinematic changes included greater hip flexion (Figure 3), knee flexion (Figure 4), and ankle dorsiflexion (Figure 5) angles throughout the gait cycle. The pelvis noticeably rotated about the longitudinal axis (Figure 6) and the anterior-posterior axis (Figure 7) to position the left hip more anterior and inferior during left foot stance. The pelvis rotation about the horizontal axis remained consistent throughout all cases (Figure 8). The hips were more externally rotated and abducted for the toeing out cases and internally rotated and adducted for the toeing in cases (Figure 9 and Figure 10). The subtalar joint angle was generally more inverted in each case compared to the experimental data (Figure 11).

The inverse dynamic analyses resulted in similar kinetic changes that correspond to the kinematic changes. The resulting kinetic changes included larger knee extensor (Figure 12) and subtalar inversion (Figure 13) torques. The hip torques showed greater internal rotation (Figure 14) and adduction (Figure 15) torques compared to the experimental data. The hip flexion torque increased with toeing in and decreased with toeing out for the wider stance cases only (Figure 16). The ankle flexion torque changes did not show significant correlation to individual cases (Figure 17).

Optimizations with Experimental Leg Torque Tracking

Similar changes, but to a lesser degree, resulted when the experimental torques were tracked. The model again flexed the hip (Figure 18), knee (Figure 19), and ankle (Figure 20) more than the experimental motion. The pelvis horizontal axis and anterior/posterior axis rotations (Figure 21 and Figure 22) along with the hip internal/external rotations (Figure 23) were similar to the prediction optimization without torque tracking. However, the pelvis longitudinal axis rotations significantly increased to aid the hip internal/external rotations (Figure 24). The subtalar motion was inverted for toeing in and everted for toeing out (Figure 25). The hip abduction/adduction motion showed a similar trend by reduced magnitude compared to the previous set (Figure 26).

Again the reduction in the knee adduction torque (Figure 27) was not greatly affected by the foot path, but was reduced for all cases (45% average decrease). However, the reduction was not as dramatic due to the limits placed on the leg torque changes. The knee flexion (Figure 28), subtalar inversion (Figure 29), and hip adduction (Figure 30) torques all increased as in the previous set. The only difference in the kinetic changes was that where the hip had a greater internal rotation torque in the previous set (Figure 14), the torque tracking set produced motions with greater hip external rotation torque (Figure 31). The hip flexion/extension and ankle torques were virtually identically in all cases including the experimental data (Figure 32 and Figure 33).

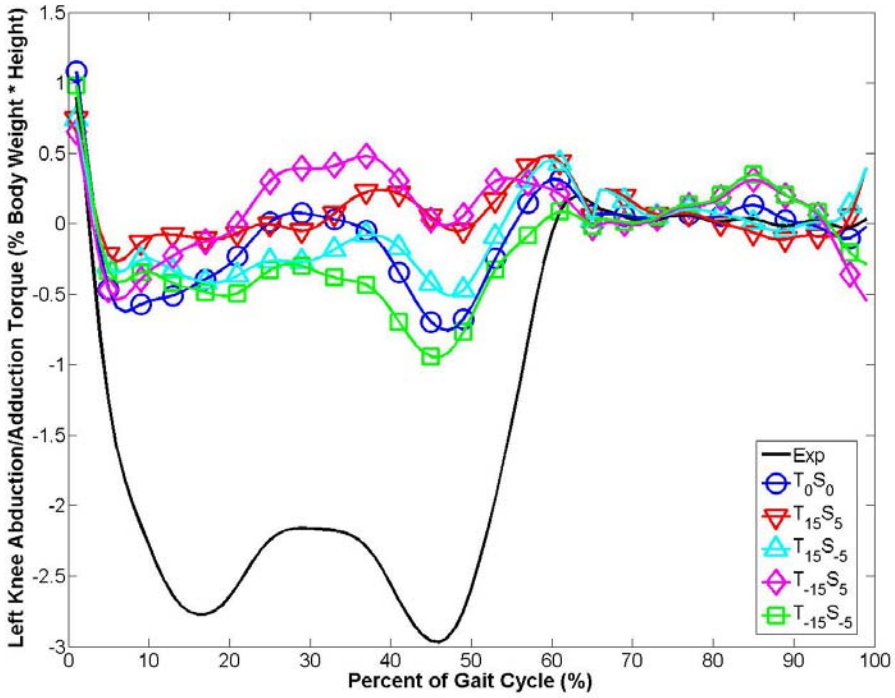

Figure 2. Comparison of left knee abduction/adduction torques achieved without matching experimental leg torques, where positive torque represents abduction and negative torque represents adduction.

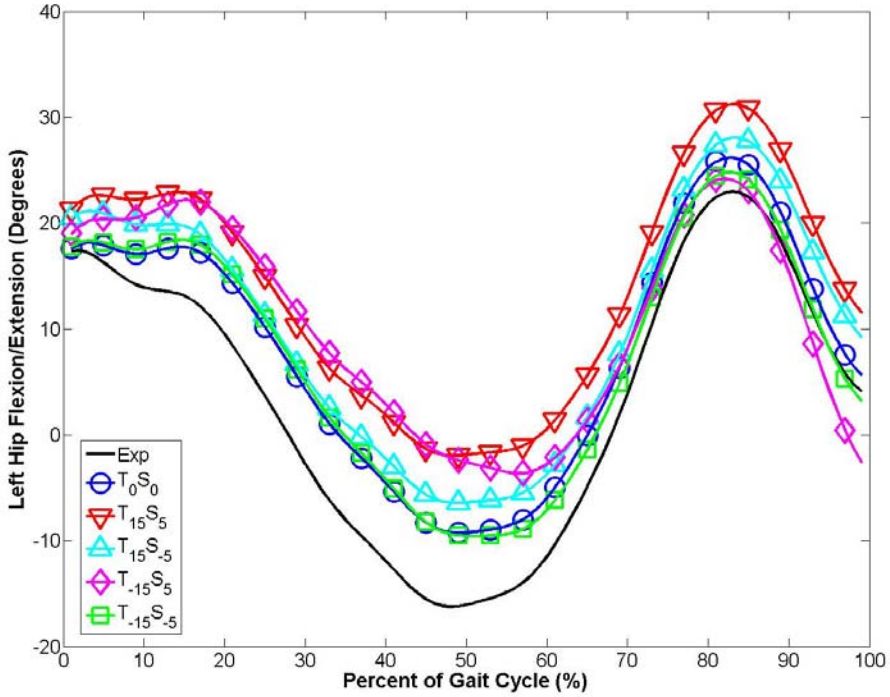

Figure 3. Comparison of left hip flexion/extension motion achieved without matching experimental leg torques, where positive angle represents flexion and negative angle represents extension.

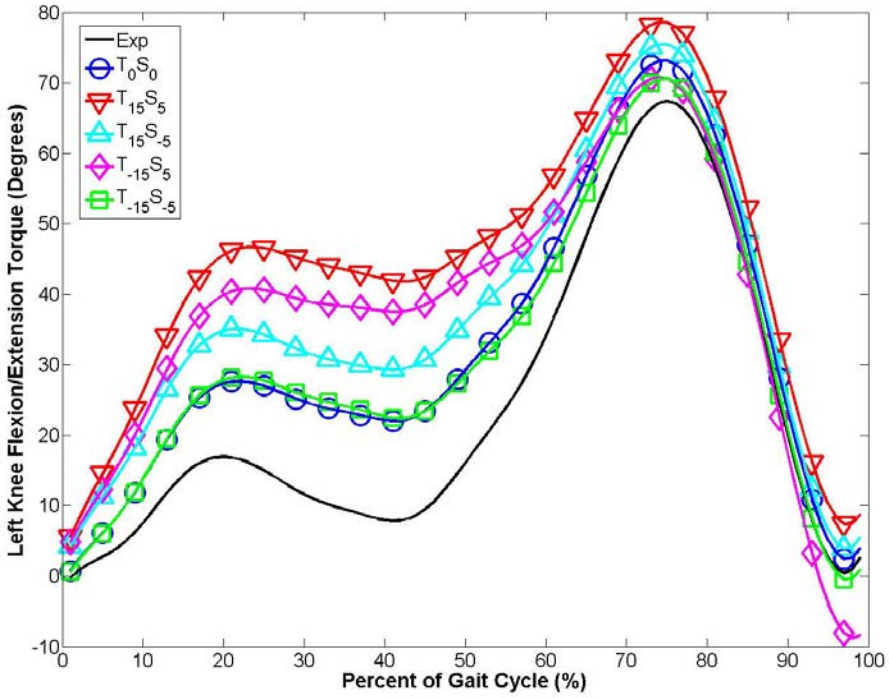

Figure 4. Comparison of left knee flexion/extension motion achieved without matching experimental leg torques, where positive angle represents flexion and negative angle represents extension.

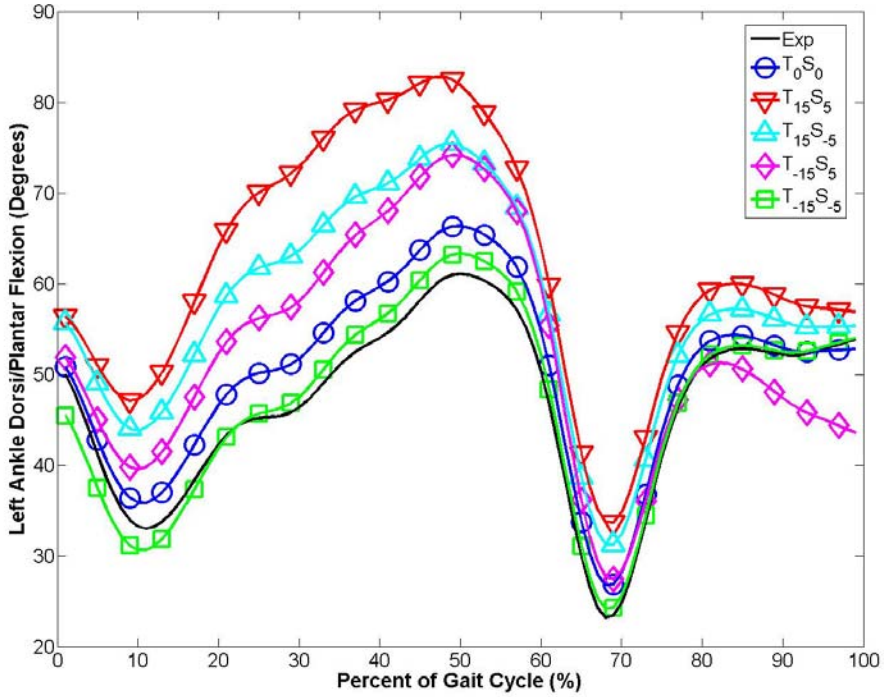

Figure 5. Comparison of left ankle dorsiflexion/planarflexion motion achieved without matching experimental leg torques, where positive angle represents dorsiflexion and negative angle represents planarflexion.

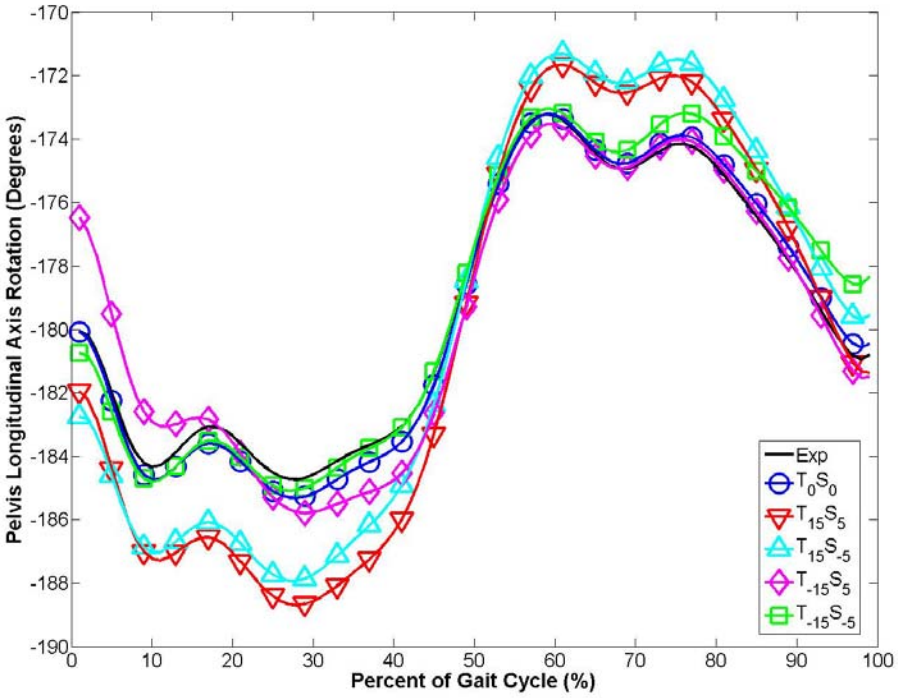

Figure 6. Comparison of pelvis longitudinal axis rotation motion achieved without matching experimental leg torques, where positive angle represents rotation to left and negative angle represents rotation to right.

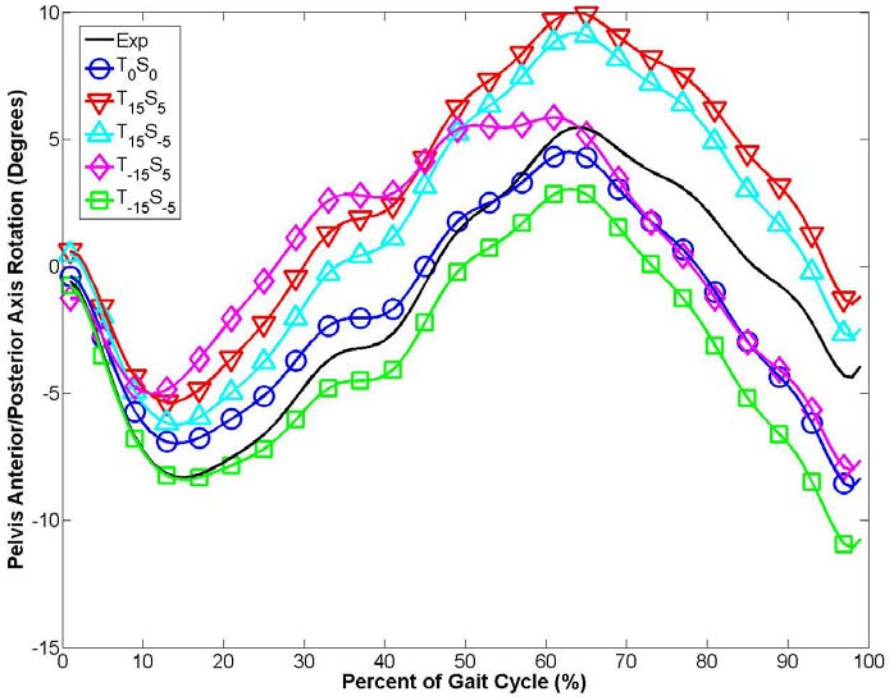

Figure 7. Comparison of pelvis anterior/posterior axis rotation motion achieved without matching experimental leg torques, where positive angle represents tilt to left and negative angle represents tilt to right.

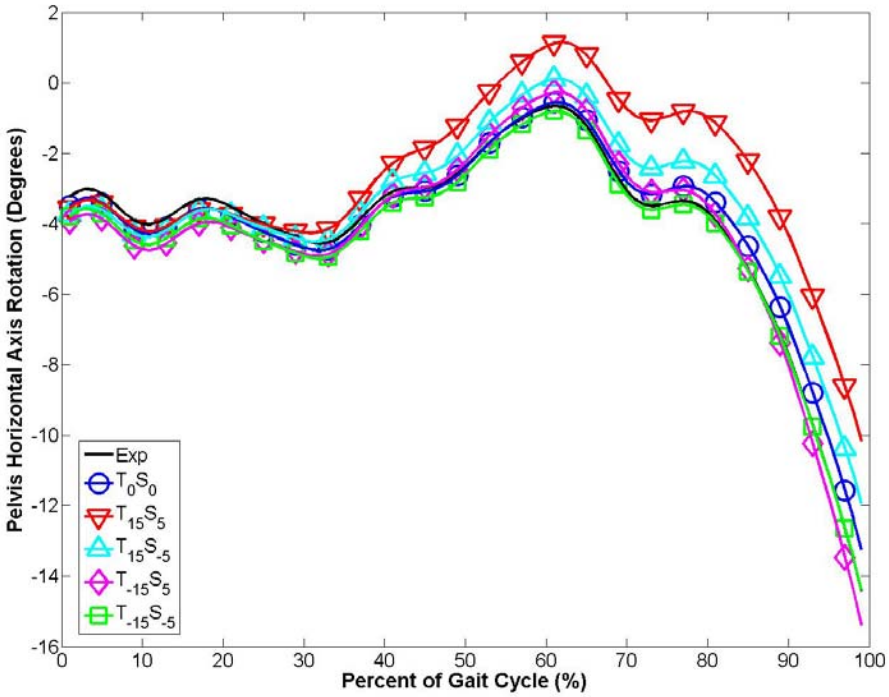

Figure 8. Comparison of pelvis horizontal axis rotation motion achieved without matching experimental leg torques, where positive angle represents forward tilt and negative angle represents backward tilt.

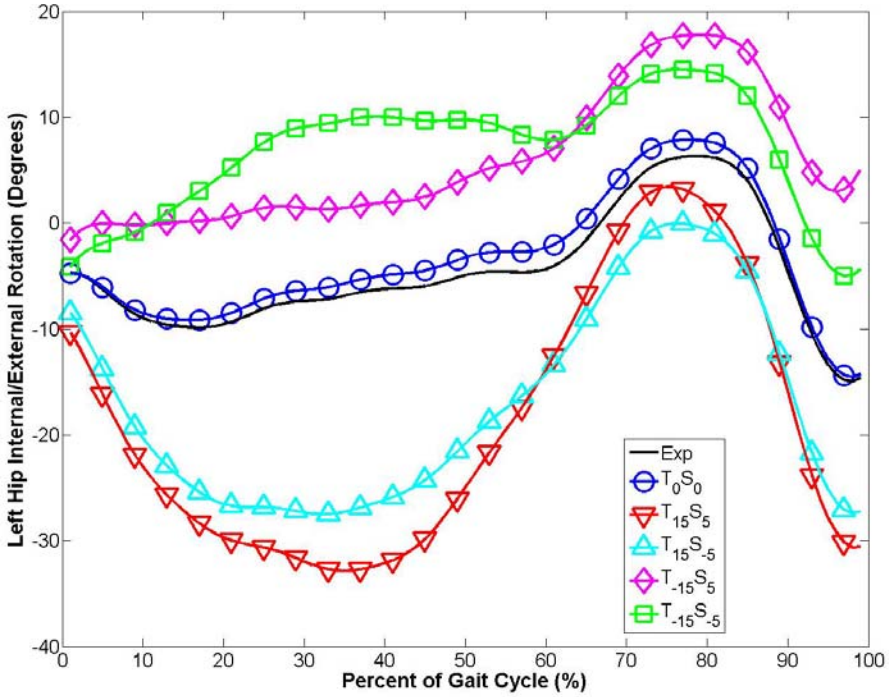

Figure 9. Comparison of left hip internal/external rotation motion achieved without matching experimental leg torques, where positive angle represents internal and negative angle represents external.

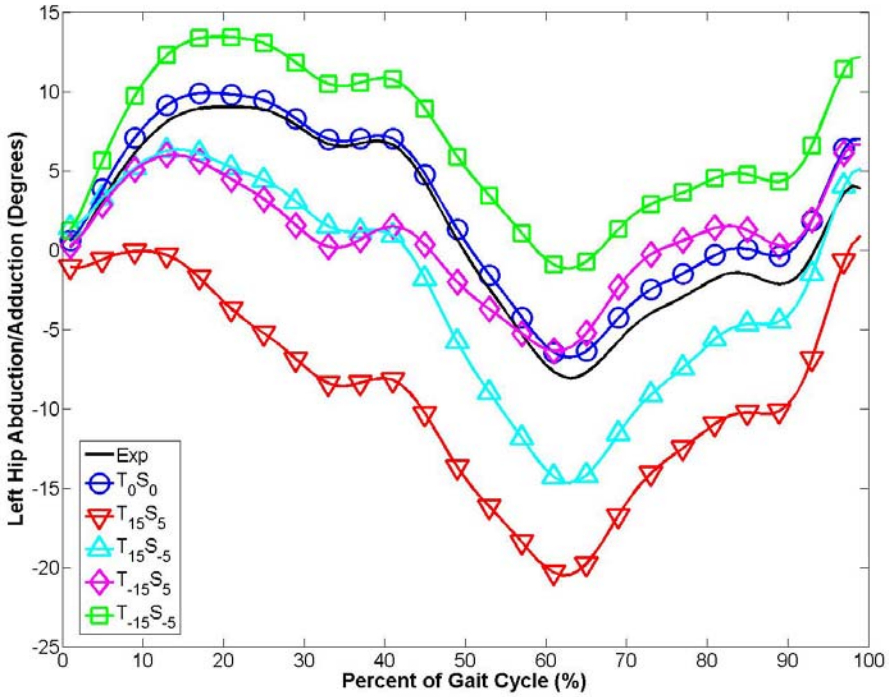

Figure 10. Comparison of left hip abduction/adduction motion achieved without matching experimental leg torques, where negative angle represents abduction and angle torque represents adduction.

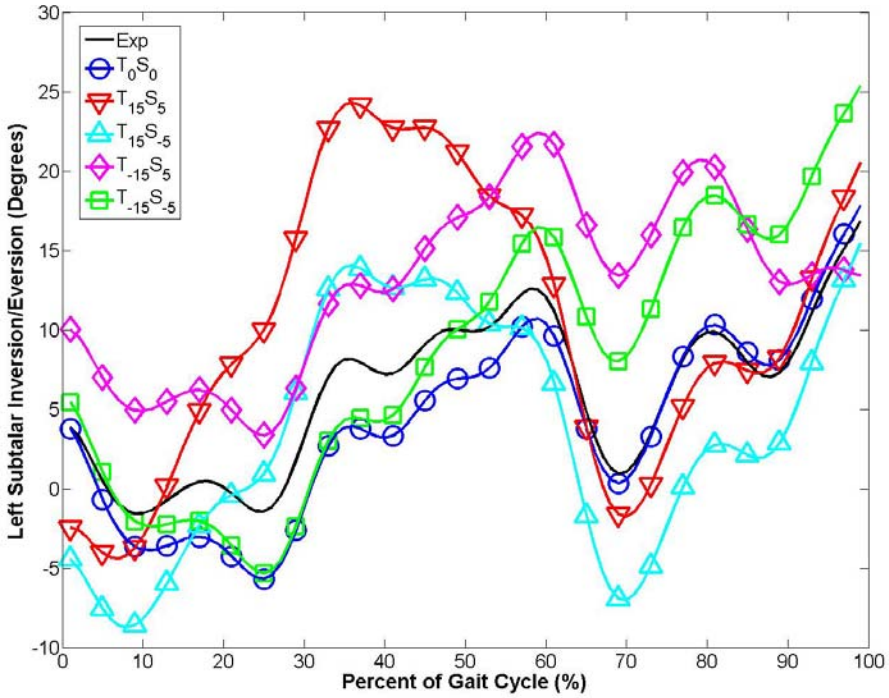

Figure 11. Comparison of left subtalar inversion/eversion motion achieved without matching experimental leg torques, where positive angle represents inversion and negative angle represents eversion.

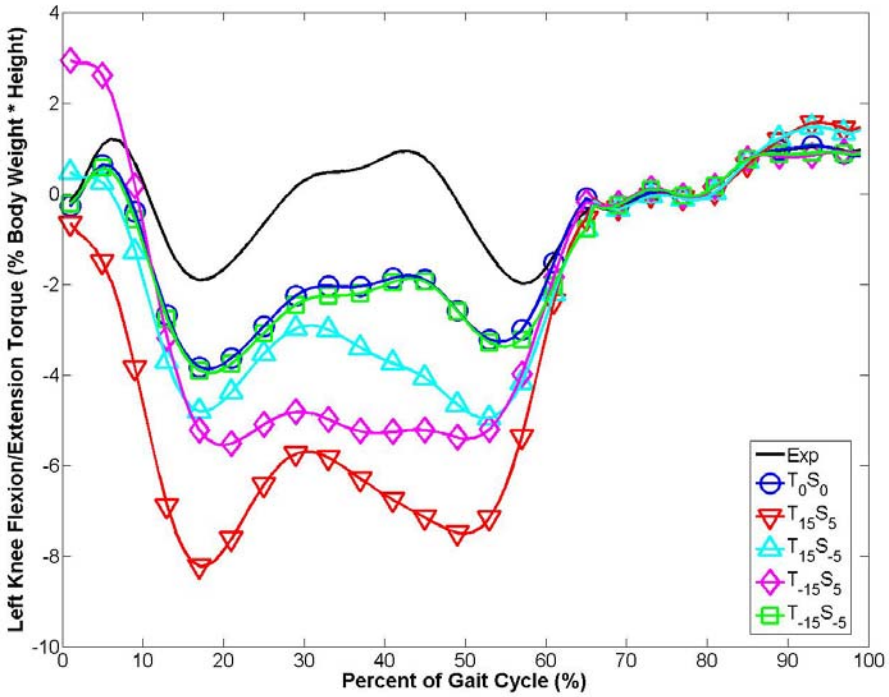

Figure 12. Comparison of left knee flexion/extension torques achieved without matching experimental leg torques, where positive torque represents flexion and negative torque represents extension.

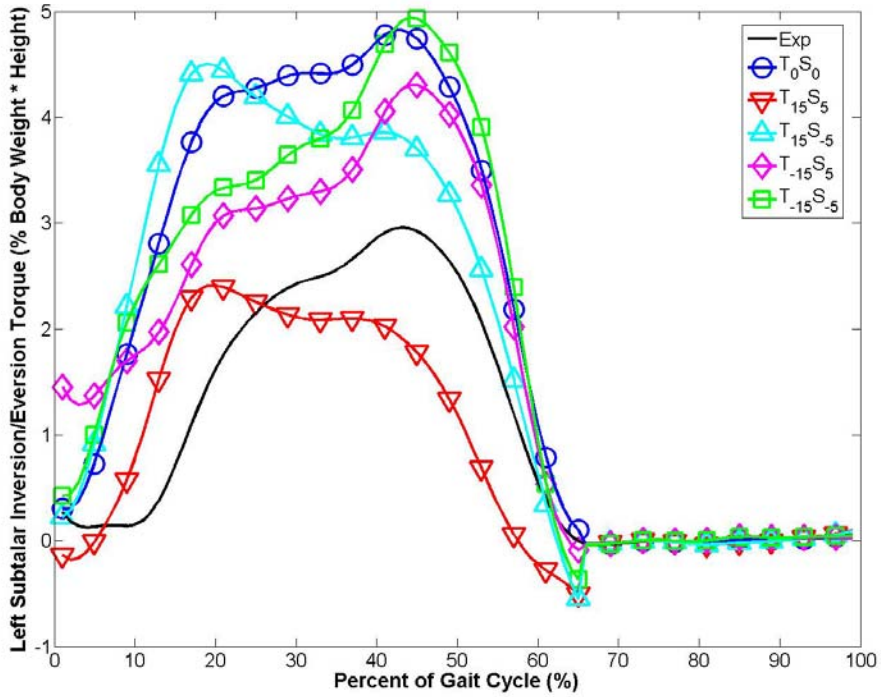

Figure 13. Comparison of left subtalar inversion/eversion torques achieved without matching experimental leg torques, where positive torque represents inversion and negative torque represents eversion.

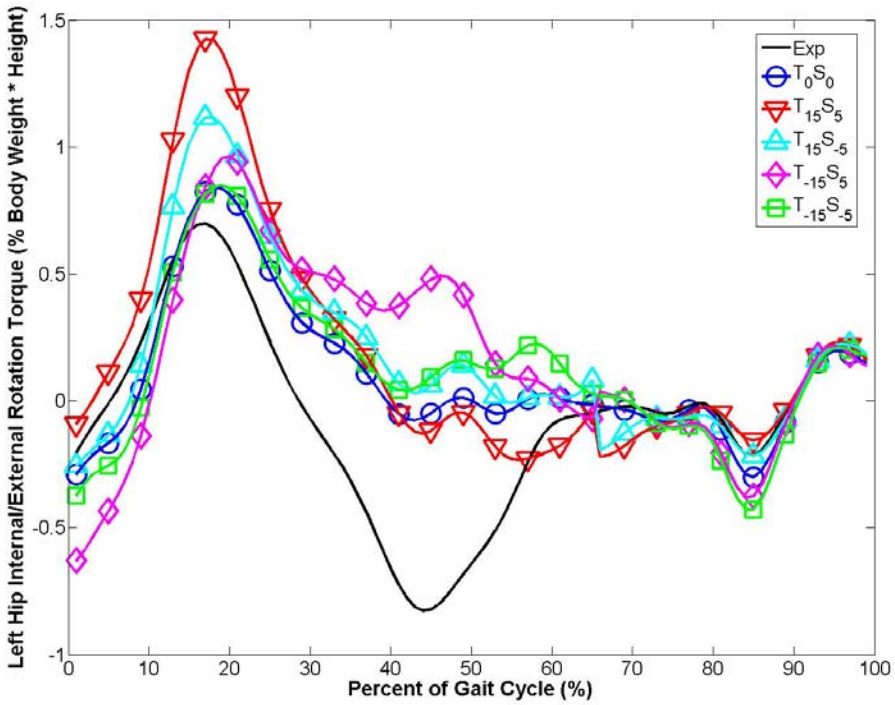

Figure 14. Comparison of left hip internal/external rotation torques achieved without matching experimental leg torques, where positive torque represents internal and negative torque represents external.

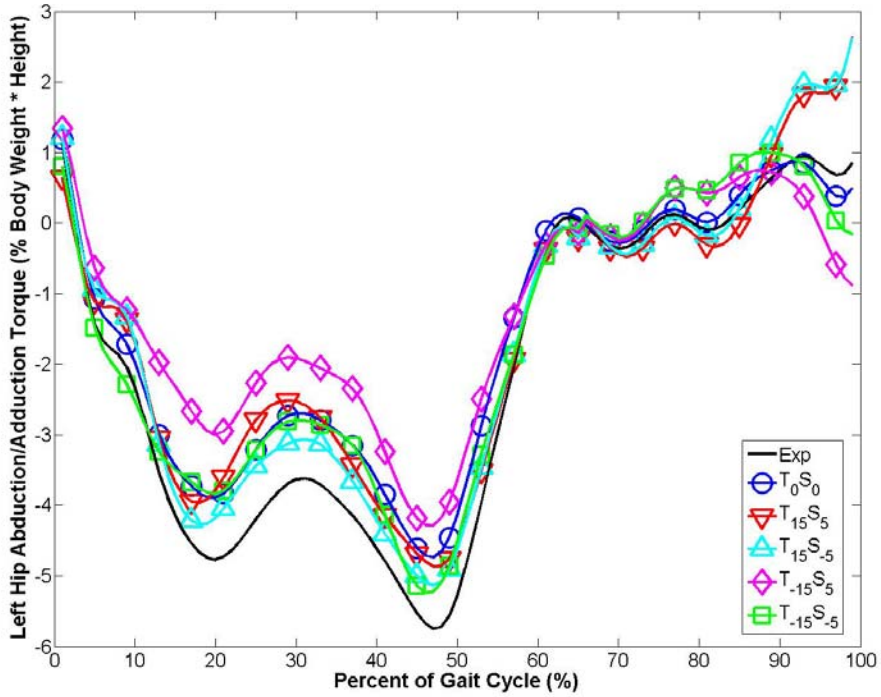

Figure 15. Comparison of left hip abduction/adduction torques achieved without matching experimental leg torques, where negative torque represents abduction and positive torque represents adduction.

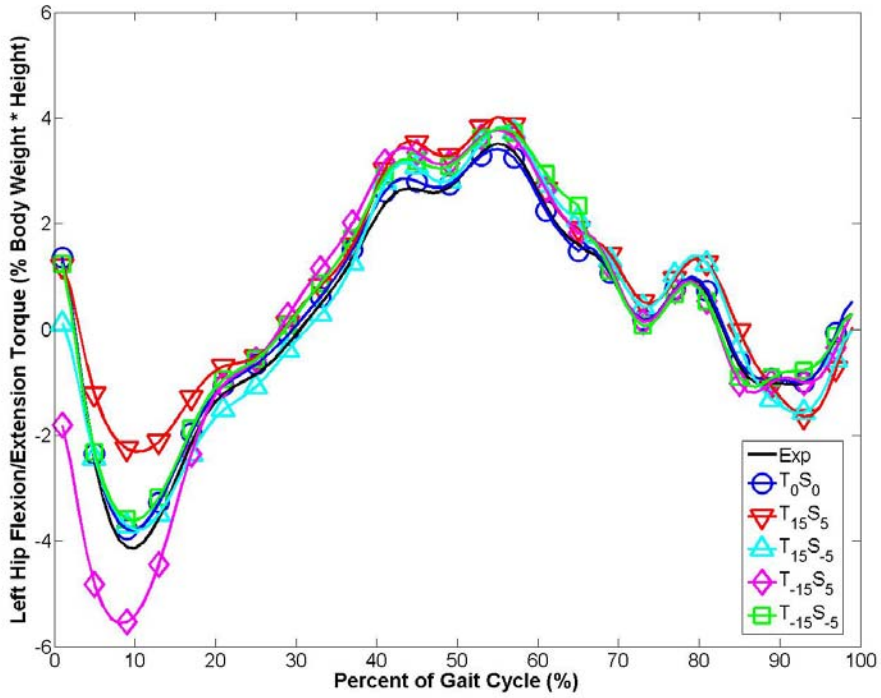

Figure 16. Comparison of left hip flexion/extension torques achieved without matching experimental leg torques, where positive torque represents flexion and negative torque represents extension.

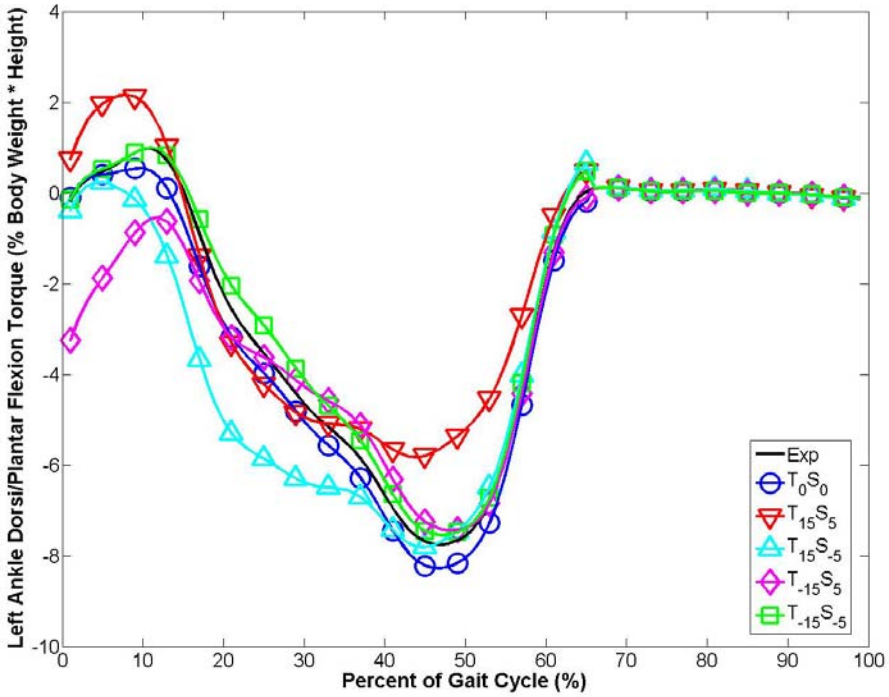

Figure 17. Comparison of left ankle dorsiflexion/planarflexion torques achieved without matching experimental leg torques, where positive torque represents dorsiflexion and negative torque represents planarflexion.

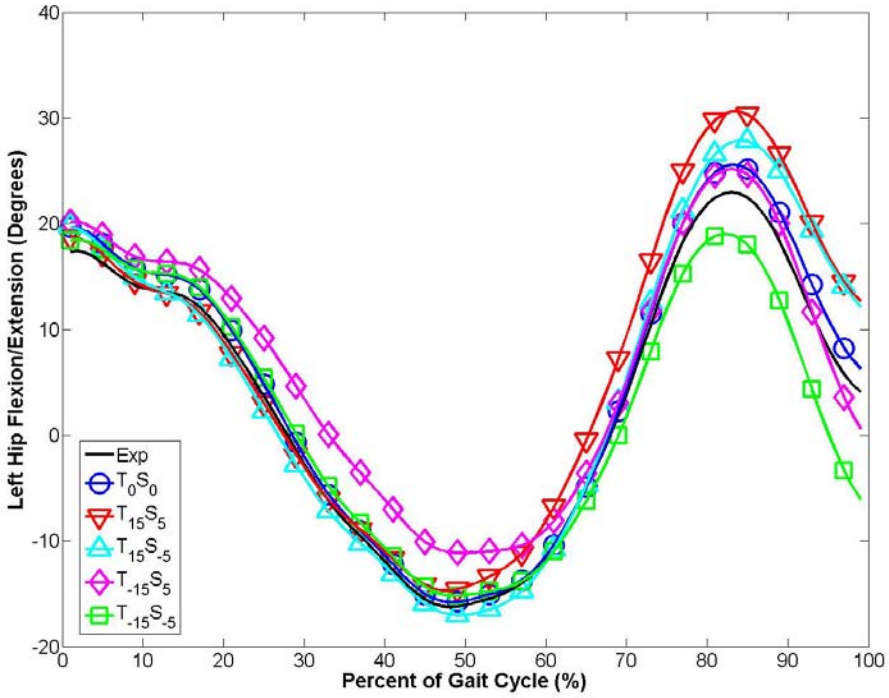

Figure 18. Comparison of left hip flexion/extension motion achieved with matching experimental leg torques, where positive angle represents flexion and negative angle represents extension.

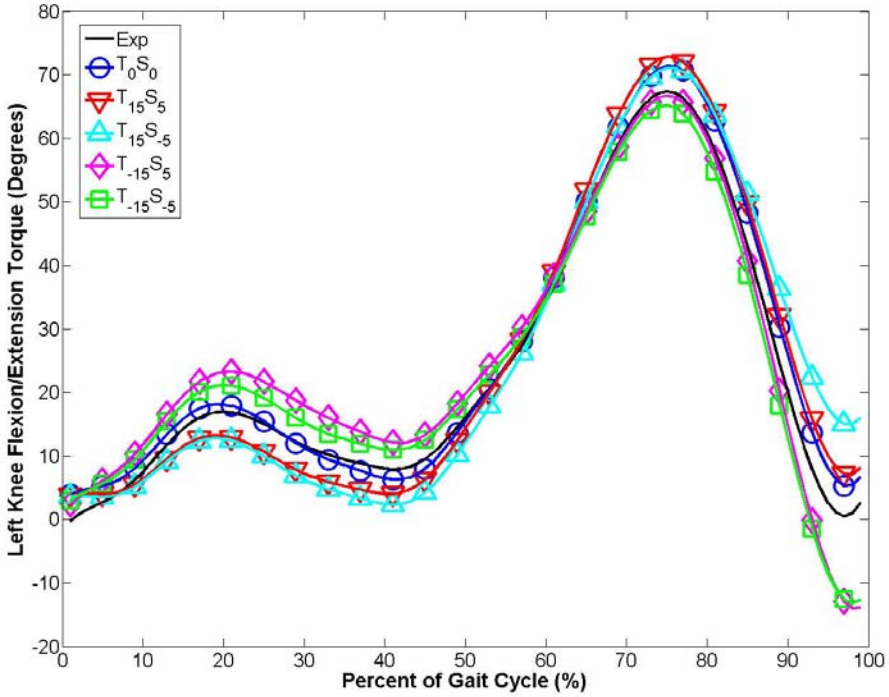

Figure 19. Comparison of left knee flexion/extension motion achieved with matching experimental leg torques, where positive angle represents flexion and negative angle represents extension.

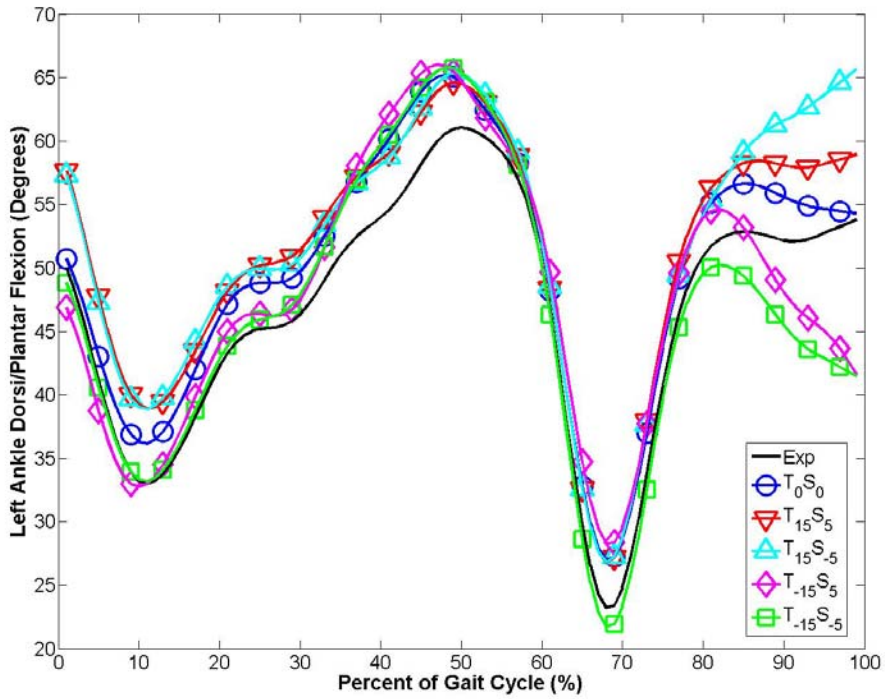

Figure 20. Comparison of left ankle dorsiflexion/planarflexion motion achieved with matching experimental leg torques, where positive angle represents dorsiflexion and negative angle represents planarflexion.

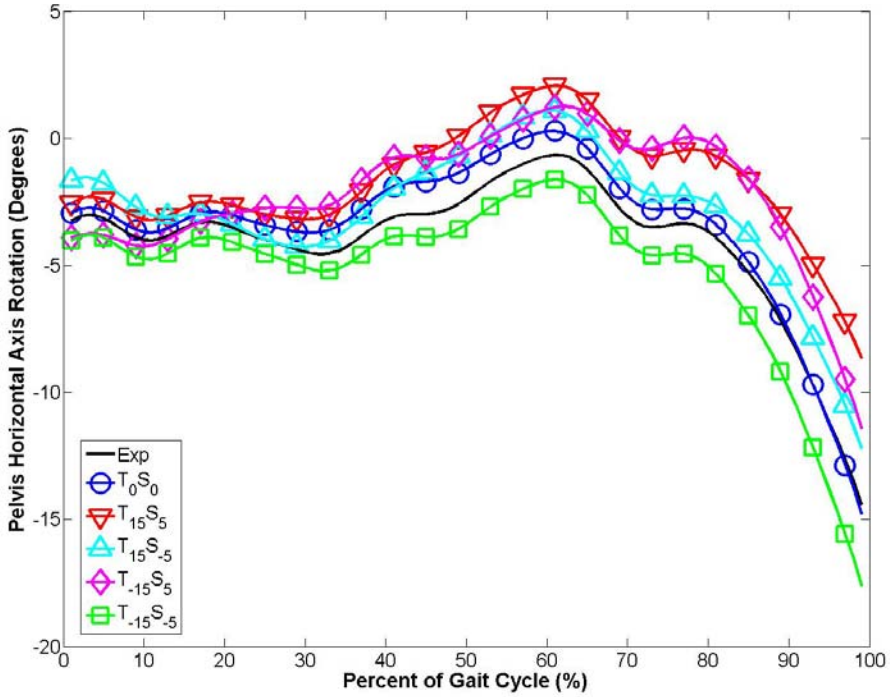

Figure 21. Comparison of pelvis horizontal axis rotation motion achieved with matching experimental leg torques, where positive angle represents forward tilt and negative angle represents backward tilt.

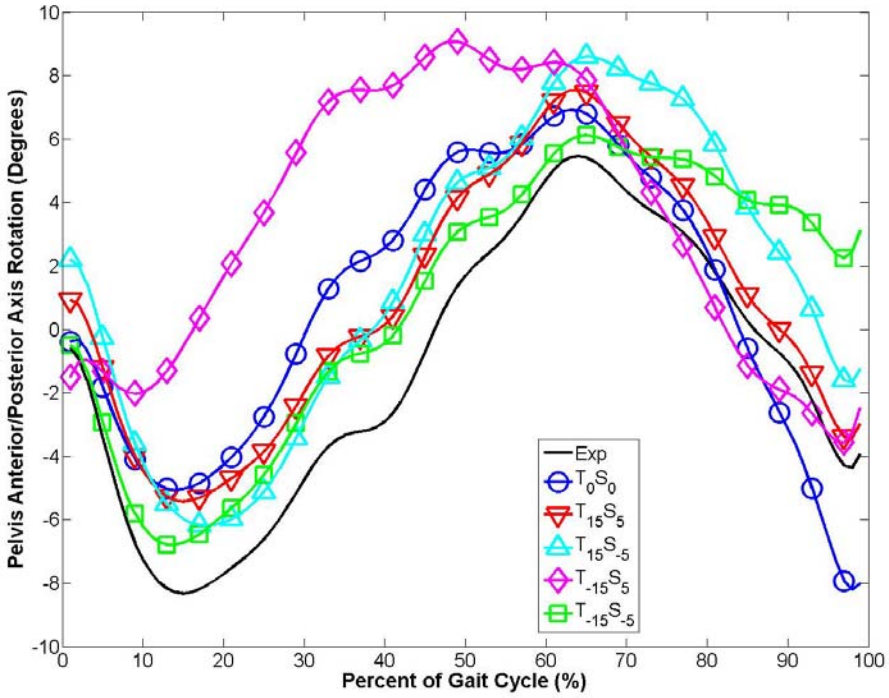

Figure 22. Comparison of pelvis anterior/posterior axis rotation motion achieved with matching experimental leg torques, where positive angle represents tilt to left and negative angle represents tilt to right.

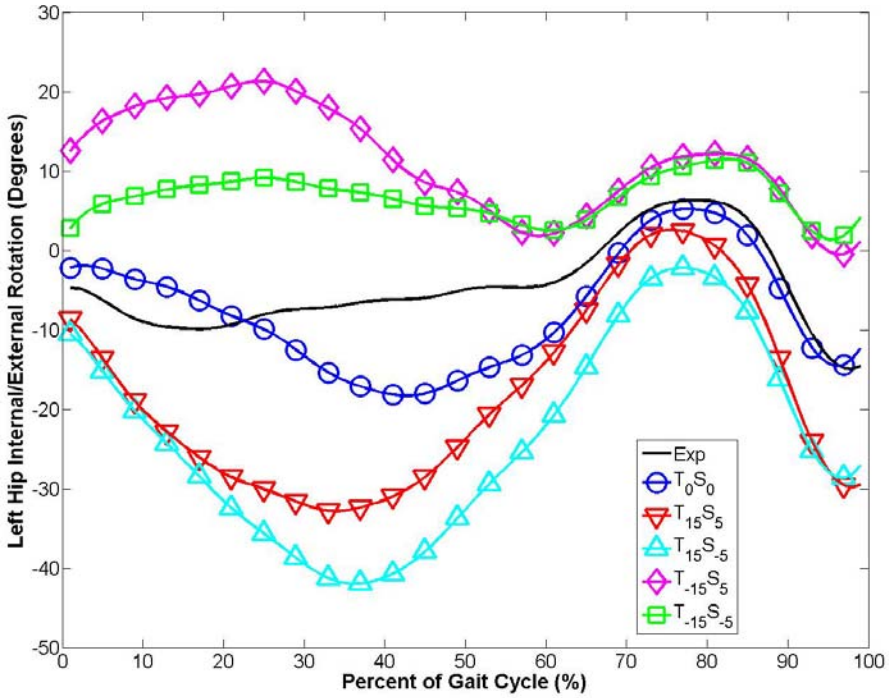

Figure 23. Comparison of left hip internal/external rotation motion achieved with matching experimental leg torques, where positive angle represents internal and negative angle represents external.

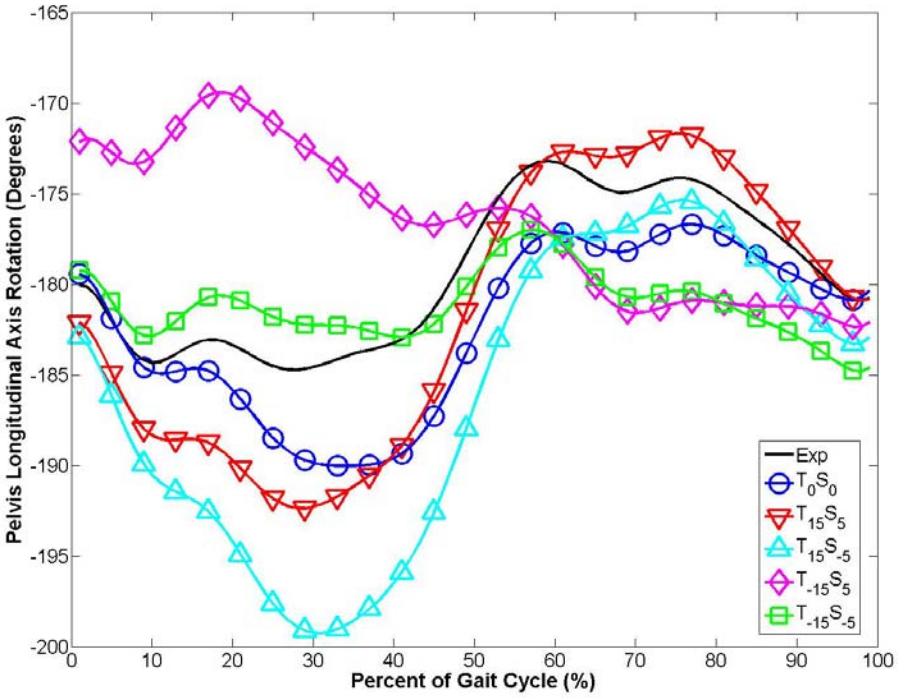

Figure 24. Comparison of pelvis longitudinal axis rotation motion achieved with matching experimental leg torques, where positive angle represents rotation to left and negative angle represents rotation to right.

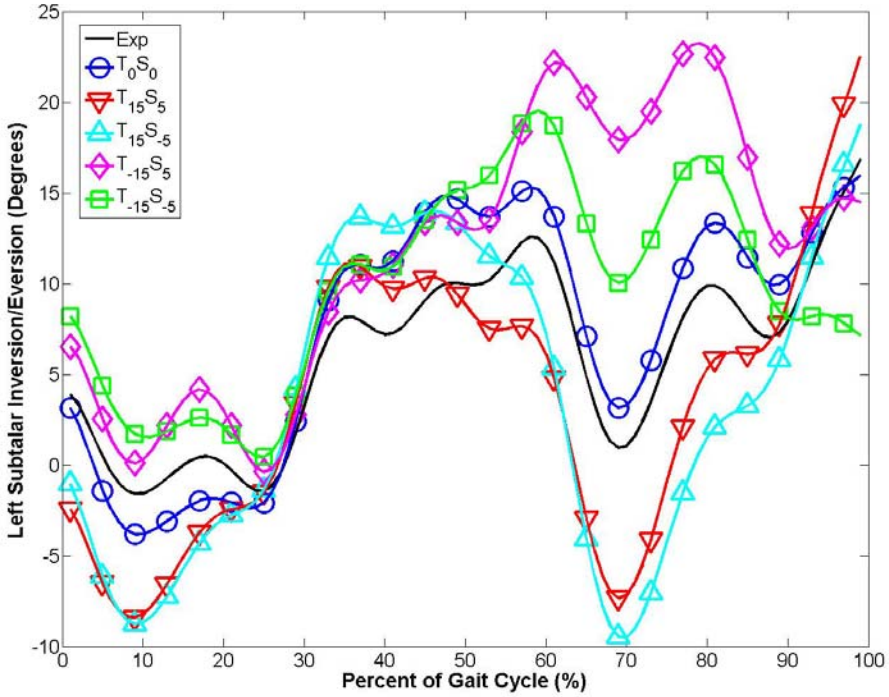

Figure 25. Comparison of left subtalar inversion/eversion motion achieved with matching experimental leg torques, where positive angle represents inversion and negative angle represents eversion.

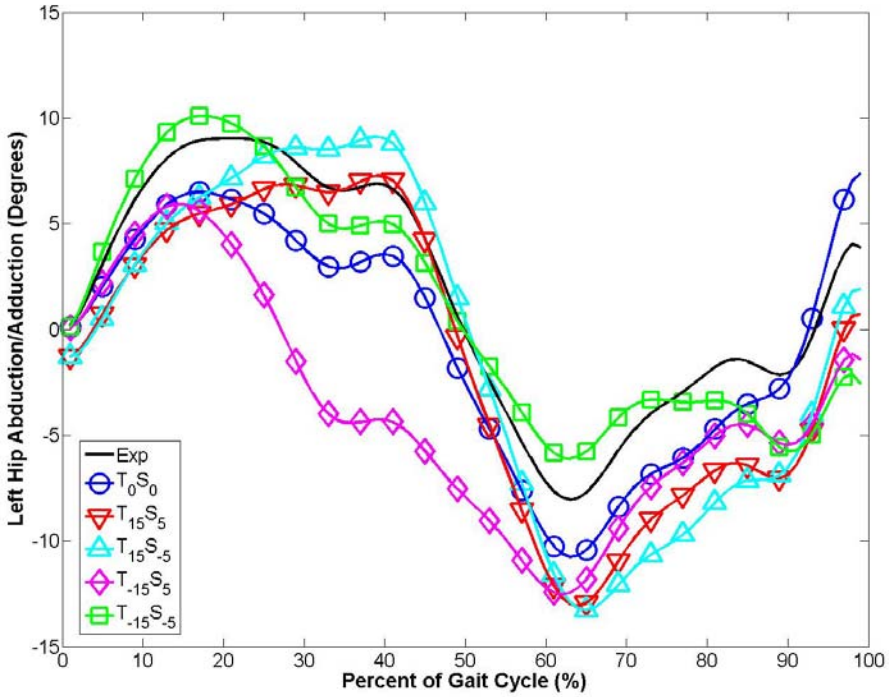

Figure 26. Comparison of left hip abduction/adduction motion achieved with matching experimental leg torques, where negative angle represents abduction and angle torque represents adduction.

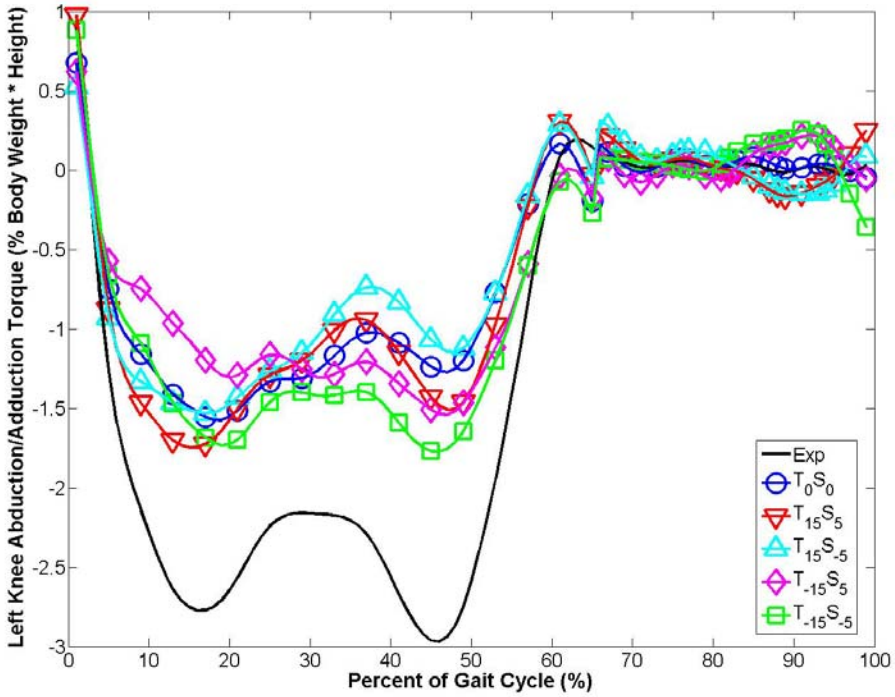

Figure 27. Comparison of left knee abduction/adduction torques achieved with matching experimental leg torques, where positive torque represents abduction and negative torque represents adduction.

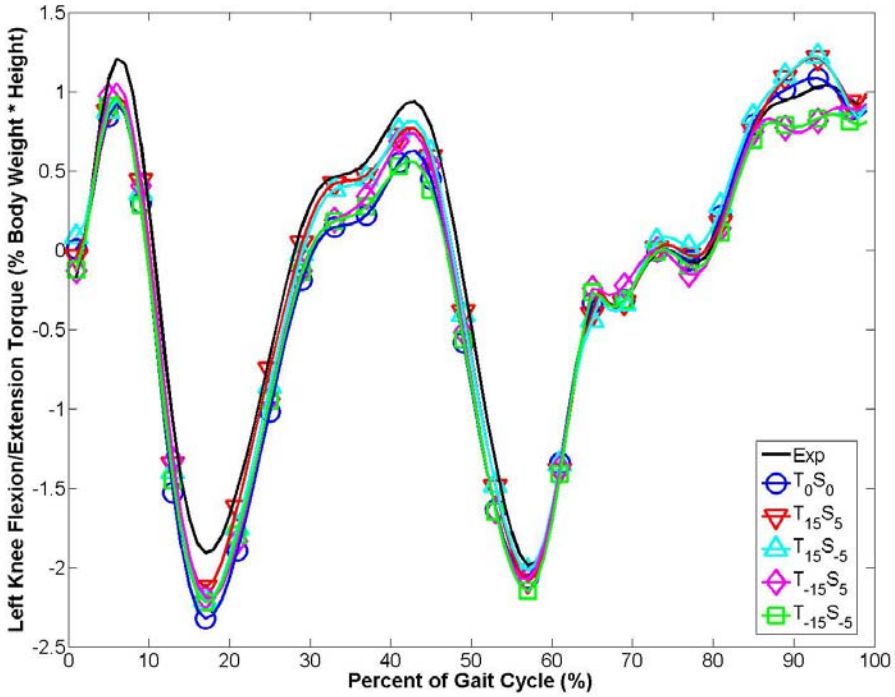

Figure 28. Comparison of left knee flexion/extension torques achieved with matching experimental leg torques, where positive torque represents flexion and negative torque represents extension.

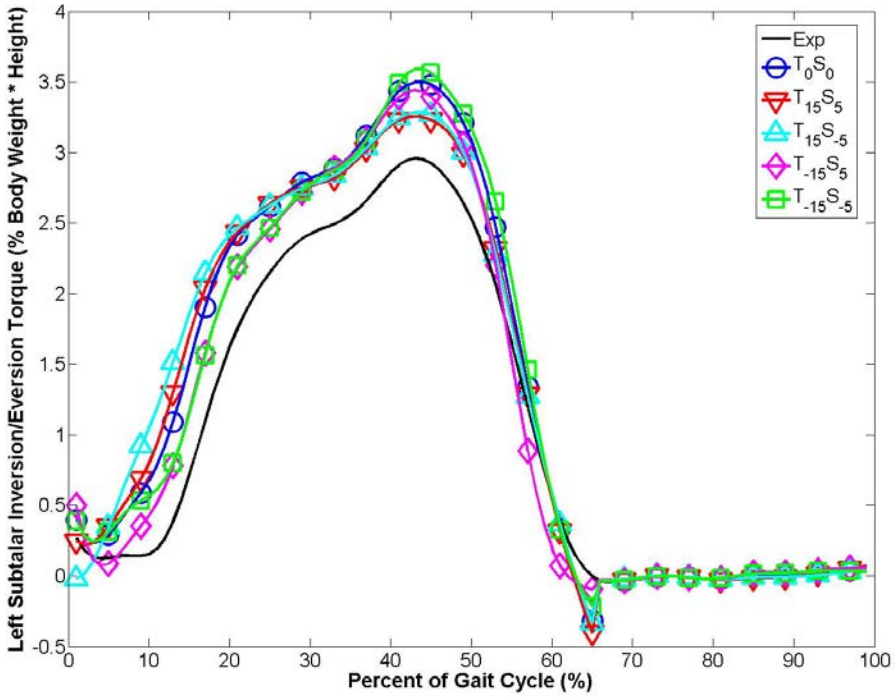

Figure 29. Comparison of left subtalar inversion/eversion torques achieved with matching experimental leg torques, where positive torque represents inversion and negative torque represents eversion.

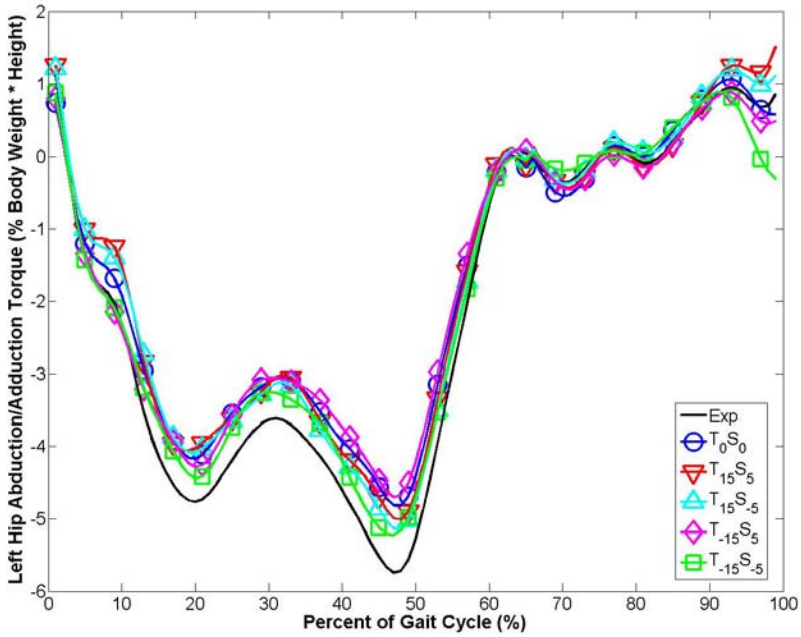

Figure 30. Comparison of left hip abduction/adduction torques achieved with matching experimental leg torques, where negative torque represents abduction and positive torque represents adduction.

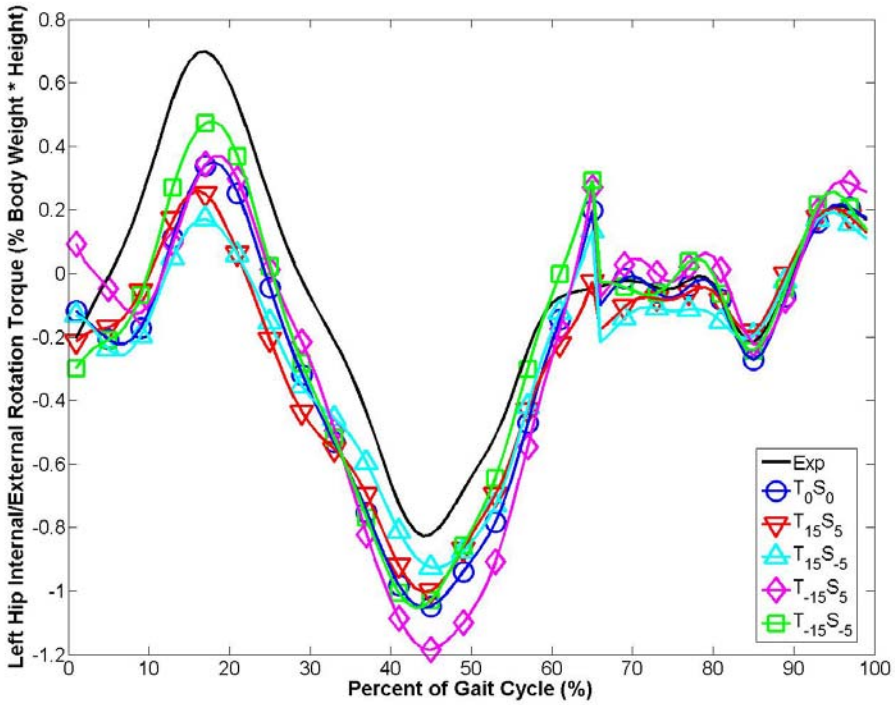

Figure 31. Comparison of left hip internal/external rotation torques achieved with matching experimental leg torques, where positive torque represents internal and negative torque represents external.

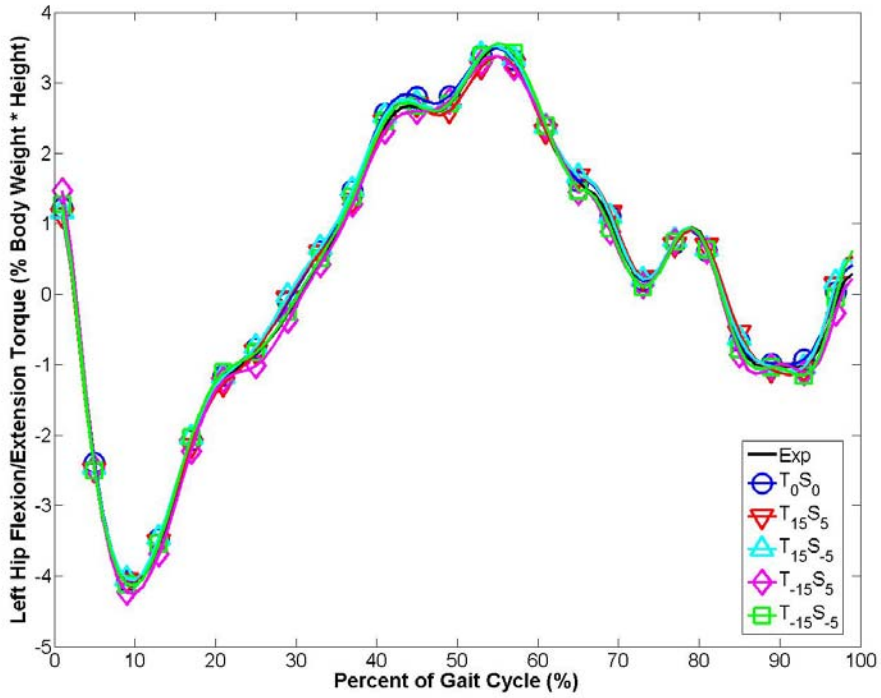

Figure 32. Comparison of left hip flexion/extension torques achieved with matching experimental leg torques, where positive torque represents flexion and negative torque represents extension.

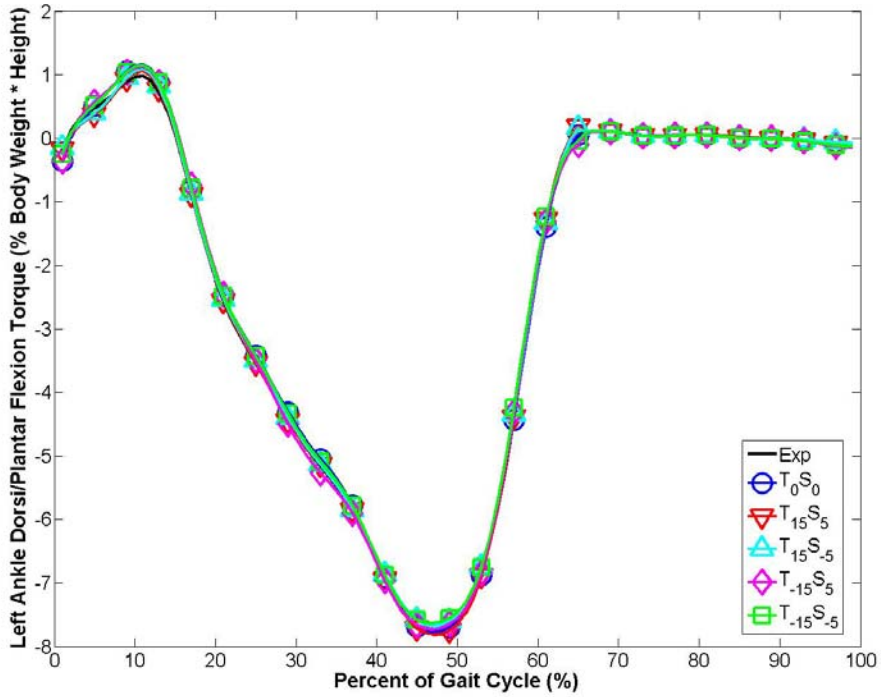

Figure 33. Comparison of left ankle dorsiflexion/planarflexion torques achieved with matching experimental leg torques, where positive torque represents dorsiflexion and negative torque represents planarflexion.

CHAPTER 5
DISCUSSION

Observations

This study used a predictive gait model to evaluate the effects of gait modifications on the knee adduction moment. An inverse dynamics optimization approach was used rather than the traditional forward dynamic approach, because of two main advantages. There are no stability problems with an inverse dynamics optimization, and inverse dynamic simulations do not require integration. Two sets of prediction optimizations were performed to determine the effect of foot placement on the knee adduction torque. The optimizations were successful in predicting novel motions that reduced the knee adduction torque, although foot placement was not a key component.

Common kinematic changes regardless of foot placement were found in all cases of the first set of optimizations that allowed unlimited torque changes. The combinations of these changes drove the left knee inward such that the ground reaction force passed through the knee more laterally resulting in a lower left knee adduction torque. The resulting kinetic changes including larger knee extensor, subtalar inversion, hip adduction, and hip internal rotation torques may not be physically possible within these joints.

The second set of prediction optimizations minimized the changes in the leg torques to avoid physically impossible solutions. Again the results for all combinations of toe out and stance width changes were similar. As in the first set of optimizations, this set also drove the left knee inward in order to reduce the adduction moment. The difference

being that many of the kinematic and kinetic changes were of a lesser degree due to the torque constraint with the exception of the pelvis longitudinal axis rotations and hip internal/external rotation torques. The combinations of kinematic changes in the second set of predication optimizations were different to allow for better tracking of the experimental torques.

Although the flexed knee motion predicted by the model was effective in reducing the adduction moment, it may be problematic for osteoarthritis patients. This motion is less energetically efficient that regular gait due to the additional knee extensor strength required to maintain the slight crouch throughout gait. Osteoarthritis patients tend to have weak knee flexors and may not be able to produce the energy required for this motion.

The resulting knee adduction torque reductions suggest that gait modifications are capable of reducing the peak knee adduction torque more than a high tibial osteotomy surgery. The average post surgery decrease for a group of 25 high tibial osteotomy patients was 34% (Prodromos *et al*., 1985). The optimizer reduced the peak knee adduction torque an average of 72% without experimental torque tracking, and 45% with torque tracking. These results are limited by the fact that this study analyzed only one patient whose experimental data showed a peak knee adduction torque close classified as normal (3% body weight * height) by Prodromos *et al*. (1985). However, the general movement modifications predicted by the optimizations suggest mechanics principles that should be applicable to any subject.

Limitations

Without including reality constraints in the cost function, the optimizer found three ideal near zero knee adduction torque results with undesired kinematics or kinetics. First, if the ground reaction forces and torques are allowed to change, the medial-lateral force

will shift more laterally. This causes the total ground reaction force to pass through the knee more laterally thus reducing the knee adduction torque without changing the motion. However, this change may not be physically realistic, because the ratio of medial-lateral to vertical forces tripled in value in order to create these ground reaction force changes. Second, if the pelvis translations are free to change, lateral pelvis swinging will result. The optimizer predicts a motion where it shifts the body's center of mass laterally by swinging the pelvis back and forth similar to a "hula" dance. As a result, the center of mass was shifted directly above the knee so that the adduction moment was near to zero. Third, if the foot path was allowed to change, the model would cross the legs during gait so as to pass one tibia through the other. As a result, the knee moved under the body's center of mass, rather than the center of mass over the knee. The runway "model walk" has the same affect on the adduction torque as the "hula walk." The "hula walk" is disadvantageous, because it is energetically inefficient. While the "model walk" does not compromise efficiency as much, there is a loss in stability by bringing the feet closer together and is not physically realizable.

CHAPTER 6
CONCLUSIONS AND FUTURE WORK

The optimizations suggest that novel movement modifications can have a significant effect on reducing the peak knee adduction torque during gait. Gait modification has a greater influence on internal knee loads than previously shown. It is interesting to note the number of different realistic motions that are able to reduce the knee adduction torque. This approach has many possibilities of clinical applications, especially for medial compartment knee osteoarthritis patients. The optimizations highlight the importance of knee extensor strength for avoiding osteoarthritis problems. As was explored in this study, these patients may be able to relieve their osteoarthritis symptoms simply by modifying their gait. Experimental evaluation of the hypothesis presented in this paper would be valuable in determining the feasibility of implementing the predicted gait modifications.

APPENDIX A
DESRIPTION OF OPTIMIZATION FILES

MATLAB FILES (See descriptions in Appendix B)

- **Call_optimizer_stance_toe.m**
- **ChangeFootPathMain.m**
- **ChangeFootPath.m**
- **Opt_min_add_grf.m**
- **Cost_func_min_add_grf.m**
- **PolyFourierFitNew.m**
- **CenterOfPressure_fourier.m**
- **Complete.m**

TEXT FILES

- **Qcoefs_Final.txt**: Fourier coefficients describing the experimental 27 DOFs.
- **Grf_coefs.txt**: Fourier coefficients describing the experimental right and left ground reaction forces and torques.
- **Kinetics_final_no_header.ktx**: A SIMM input file, which contains the experimental positions, velocities, accelerations, and ground reactions.
- **Invdyn_foot_exp_final.txt**: The foot, trunk and pelvis path calculated by the executable with the experimental data.
- **Invdyn_trq_exp_final.txt**: The inverse dynamic torques calculated by the executable with the experimental data.
- **Params.txt:** A text file read by the executable where the user must specify the name if the input kinetics file and desired step size for output data.

OTHER

- **Simulation.exe**: The executable that performs inverse dynamics given an input kinetics file.

- **Msvcr71d.dll**: A library file needed to run the executable

APPENDIX B
DESCRIPTION OF MATLAB FILES

Matlab Files	Called by	Inputs	Outputs	Description
Call_optimizer_ stance_toe.m.m	User	None	Coefficients_guess .txt Kinetics_guess.ktx	Calls the optimization function. Change the foot placement values here to predict a different motion.
ChangeFootPathMai	Call_optimizer _stance_toe.m	Foot placement variables, invdyn_exp_final.txt kinetics_final_no_header.ktx	Invdyn_foot_chan ged.txt	Calculates the changes in the x,y,z foot translations and rotations with respect to the ground frame.
ChangeFootPath.m	ChangeFootPat hMain.m	Old translations and rotations and changed to foot path translations and rotations.	New foot translations and rotations.	Calculates the new x,y,z foot translations and rotations with respect to the ground frame.
Opt_min_add_grf.m	Call_optimizer _stance_toe.m	invdyn_foot_exp_final.txt, invdyn_foot_changed.txt, invdyn_trq_exp_final.txt, kinetics_final_no_header.ktx, QCoefs_Final.txt grf_coefs.txt	None	Loads experimental values. Creates initial conditions matrix. Calls the Matlab optimizer, “lsqnonlin.”
Cost_func_min_ add_grf.m	Opt_min_add_ grf.m	Current guess of design variables, invdyn_trq.txt invdyn_foot.txt cop_error.txt	Cost function error matrix, to be squared and summed by the optimizer.	Reads in the current guess of the design variables. Writes a kinetics file based on that guess. Calls simulation.exe. Reads in inverse dynamic results. Calculates cost function.
PolyFourierFitNew.	Cost_func_min _add_grf.m	Fourier coefficients, omega, time, degree of polynomial, derivative flag	Values of the curves at the specified time points.	Creates motion and ground reaction curves based on the Fourier coefficients.
CenterOfPressure_ fourier.m	Cost_func_min _add_grf.m	Ground reaction forces and torques in the ground reference frame.	Center of pressure locations in the ground reference frame.	Calculates the left and right centers of pressure in the ground reference frame.
Complete.m	Opt_min_ add_grf.m	None	None	Alerts user when an optimization has terminated.

LIST OF REFERENCES

Anderson, F.C., Pandy, M.G. (2001). Dynamic Optimization of Human Walking. Journal of Biomechanical Engineering 123, 381-390.

Andriacchi, T.P. (1994). Dynamics of Knee Malalignment. Orthopedic Clinics of North America 25, 395-403.

Arnold, A.S., Blemker, S.S., Delp, S.L. (2001). Evaluation of a Deformable Musculoskeletal Model for Estimating Muscle-Tendon Lengths During Crouch Gait. Annals of Biomedical Engineering 29, 263-274.

Delp, S.L., Loan, J.P., Hoy, M.G., Zajac, F.E., Topp E.L., Rosen, J.M. (1990). An Interactive Graphics-based Model of the Lower Extremity to Study Orthopaedic Surgical Procedures. IEEE Transactions on Biomedical Engineering 37, 757-767.

Delp, S.L., Arnold, A.S., Speers, R.A., Moore, C.A. (1996). Hamstrings and Psoas Lengths During Normal and Crouch Gait: Implications for Muscle-Tendon Surgery. Journal of Orthopaedic Research 14, 144-151.

Gerristen, K.G.M., van den Bogert, A.J., Hulliger, M., Zernicke, R.F. (1998). Intrinsic Muscle Properties Facilitate Locomotor Control – A Computer Simulation Study. Motor Control 2, 206-220.

Hurwitz, D.E., Ryals, A.R., Block, J.A., Sharma, L., Shcnitzer, T.J., Andriacchi, T.P. (2000). Knee Pain and Joint Loading in Subjects with Osteoarthritis of the Knee. Journal of Orthopaedic Research 18, 572-579.

Pandy, M.G. (2001). Computer Modeling and Simulation of Human Movement. Annual Reviews in Biomedical Engineering 3, 245-273.

Prodromos, C.C., Andriacchi, T.P., Galante, J.O. (1985). A Relationship between Gait and Clinical Changes following High Tibial Osteotomy. The Journal of Bone and Joint Surgery 67A, 1188-1194.

Sharma, L., Hurwitz, D.E., Thonar, E.J-M.A., Sum, J.A., Lenz, M.E., Dunlop, D.D., Schnitzer, T.J., Kirwan-Mellis, G., Andriacchi, T.P. (1998). Knee Adduction Moment, Serum Hyaluronan Level, and Disease Severity in Medial Tibiofemoral Osteoarthritis. Arthitis & Rheumatism 41, 1233-1240.

Wang, J.W., Kuo, K.N., Andriacchi, T.P., Galante, J.O. (1990). The Influence of Walking Mechanics and Time on the Results of Proximal Tibial Osteotomy. Journal of Bone and Joint Surgery 72A, 905-913.

Winter, D.A. (1990). Biomechanics and Motor Control of Human Movement, 2nd Edition. Wiley, New York.

BIOGRAPHICAL SKETCH

Kelly Rooney was born in Michigan in 1979. She moved to Palm Harbor, Florida, with her family in 1986 and remained there through the completion of her high school education. She graduated valedictorian from East Lake High School in 1997 and began her studies at The University of Florida that fall. Kelly graduated with a Bachelor of Science degree in engineering science in May of 2002. In addition to her major studies, she also received minors in biomechanics, French and music. She continued her education at the University of Florida as a graduate student in the Department of Biomedical Engineering in August 2002. Throughout her stay at the University of Florida, Kelly has been very active in three sport clubs. She has served as the president and captain of the Women's Roller Hockey Club, and competed nationally with Team Florida Cycling and the Tri-Gators triathlon club.